# Material properties dependent on the thermal transport in a cylindrical nanowire*

Zhang Yong(张 勇)[a], Xie Zhong-Xiang(谢忠祥)[a]†, Deng Yuan-Xiang(邓元祥)[a], Yu Xia(喻 霞)[a]‡, and Li Ke-Min(李科敏)[b]

[a] *Department of Mathematics and Physics, Hunan Institute of Technology, Hengyang* 421002, *China*
[b] *Department of Physics and Electronics Information, Hunan Institute of Science and Technology, Yueyang* 414004, *China*

(Received 23 April 2015; revised manuscript received 4 August 2015; published online 20 October 2015)

Using the elastic wave continuum model, we investigate the effect of material properties on ballistic thermal transport in a cylindrical nanowire. A comparative analysis for the convexity-shaped and concavity-shaped structure is made. It is found that in the convexity-shaped structure, the material with higher wave velocity in the convexity region can increase the thermal conductance at the lower temperature range; the thermal conductance of the nanowire with higher wave velocity in the convexity region is lower than that of the nanowire with lower wave velocity in the convexity region at the higher temperature range. However, in the concavity-shaped structure, the material properties of the concavity region have less effect on the thermal conductance at the lower temperature range; the material with higher wave velocity in the concavity region can reduce the thermal conductance at the higher temperature range. A brief analysis of these results is given.

**Keywords:** acoustic phonon transport, nanostructure, transmission coefficient, thermal conductance

**PACS:** 63.22.–m, 73.23.Ad, 44.10.+i **DOI:** 10.1088/1674-1056/24/12/126302

## 1. Introduction

In recent years, thermal properties associated with acoustic phonons in semiconductor nanostructures have attracted a great deal of attention.[1–8] Employing the Landauer formulation of transport theory, Rego *et al.*[9] firstly predicted the existence of thermal conductance quantization, $\pi^2 k_B^2 T/3h$, analogous to the well-known $2e^2/h$ electronic conductance quantization, in the dielectric quantum wire with catenoid contacts between the wire and the reservoirs at low temperatures. This prediction has been verified by Schwab *et al.*[10] Understanding thermal conductivity of the nanostructure is very critical to address power dissipation in a nanodevice, which is one of the important problems faced by current electronic miniaturization. Materials with higher thermal conductivity are needed to solve the serious heat dissipation in ever-smaller integrated circuits, while materials with lower thermal conductivity are required to improve the thermal insulation in high-power engines and for achieving high thermoelectric efficiency. For this purpose, various methods in nanostructures including nanowires,[11–17] nanotubes,[18–21] and nanobelts[22–25] are proposed to regulate thermal conduction. Now, the methods of thermal conduction regulation can be classified into two groups. One group tailors thermal conductance through designing various structural discontinuities,[26–29] the other group regulates the phonon scattering strength by introducing point scatterers, such as impurities and substitutions.[30,31] Using molecular dynamic method, Liu *et al.*[32] investigated that the effect of isotopic doping on the thermal conductance of silicene nanosheets, finding that isotopic doping can reduce the thermal conductivity at low temperatures. Chen *et al.*[26] explored how different types of defects affect the thermal conductance in the rectangular nanowire at low temperatures, finding that some defects can reduce the thermal conductance. Recently, material properties of two coupled nanocavities on the thermal conductance in a two-dimensional nanowire are also investigated at low temperatures.[33]

In the present work, we investigate the effect of material properties on ballistic phonon transmission and thermal conductance in a cylindrical nanowire at low temperatures by applying the elastic wave continuum model method. To the best of our knowledge, only rectangular geometries are considered in previous studies. However, the thermal transport properties in a cylindrical semiconductor nanowire are paid very little attention. Generally, cylindrical structures can be used more widely in experimental measurement and potential applications compared to rectangular structures. Our results show that in the zero temperature limit, the quantum value $\pi^2 k_B^2 T/3h$ of the thermal conductance can be observed in all cases, even when the phonon-scattering is introduced. Moreover, this quantization is independent of the variation of the material properties. When the temperature is increased, the quantum platform of the thermal conductance is destroyed,

*Project supported by the National Natural Science Foundation of China (Grant No. 11404110), the Natural Science Foundation of Hunan Province, China (Grant Nos. 14JJ3139, 2015JJ6027, and 2015JJ6030), the Outstanding Young Program from the Education Department of Hunan Province, China (Grant No. 14B046), and the Doctoral Activation Foundation of Hunan Institute of Technology of China (Grant No. HQ14006).

†Corresponding author. E-mail: xiezxhu@163.com
‡Corresponding author. E-mail: yuxia83@126.com

© 2015 Chinese Physical Society and IOP Publishing Ltd 

and the thermal conductance firstly increases to the minimum value, then increases. These are qualitatively in agreement with the experimental results by Schwab *et al.*[10]

This paper is organized as follows. In Section 2, we give a brief description of the model and the formulas used in calculations. In Section 3, we numerically discuss the phonon transmission coefficient and thermal conductance. Finally, we summarize our results in Section 4.

## 2. Model and method

We consider the model structure shown in Fig. 1, a cylindrical semiconductor nanowire is connected by a scattering region with different materials. Here, we suppose that the temperatures in regions I and III are $T_{\rm L}$ and $T_{\rm R}$, respectively. The temperature difference $\delta T$ ($\delta T = T_{\rm L} - T_{\rm R}$) is so small that we can use the mean temperature $T$ [$T = (T_{\rm L} + T_{\rm R})/2$] as the temperature of region I and III in the following calculation. The formula of thermal conductance in the ballistic region can be written as:[26]

$$K = \frac{\hbar^2}{k_{\rm B}T^2}\sum_m \frac{1}{2\pi}\int_{\omega_m}^{\infty}\tau_m(\omega)\frac{\omega^2 {\rm e}^{\beta\hbar\omega}}{({\rm e}^{\beta\hbar\omega}-1)^2}{\rm d}\omega, \tag{1}$$

where $\omega_m$ is the cutoff frequency of the $m$-th mode; $\beta = 1/(k_{\rm B}T)$, where $k_{\rm B}$ and $T$ are the Boltzmann constant and temperature, and $\hbar$ is Planck's constant, respectively. $\tau_m(\omega)$ is the energy transmission coefficient of the $m$-th mode at frequency $\omega$ from region I across all the interfaces into region III, which is the key issue to calculate $\tau_m(\omega)$.

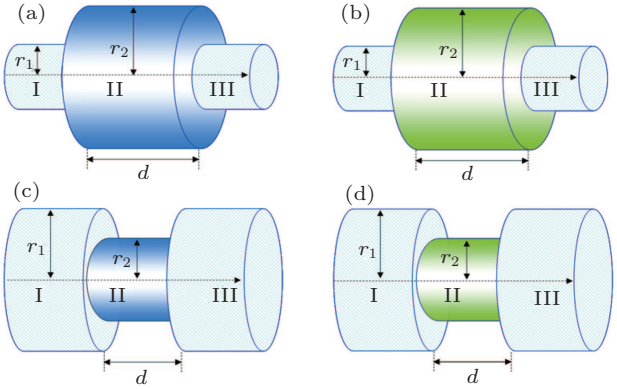



**Fig. 1.** (color online) Schematic diagram for two semi-infinite cylindrical nanowires with an embedded abrupt scattering region made of different materials. Panels (a) and (b) correspond to the convexity-shaped structure with GaAs and AlAs convexity region, panels (c) and (d) correspond to the concavity-shaped structure with GaAs and AlAs concavity region, respectively.

At low temperatures, ballistic phonon wavelengths are generally over several hundreds of angstroms, which are much greater than the dimensions of the structure. Naturally, microscopic length such as the atomic bond length is much smaller than the wavelength of the ballistic phonon. Thus, we use the elastic wave continuum model to describe the ballistic phonon propagation in this work. In the elastic approximation, the phonon displacement $U(r,\theta,z)$ in the cylindrical coordinate satisfies the following equation:

$$v^2\nabla^2 U + \omega^2 U = 0, \tag{2}$$

where $v = \sqrt{C_{44}/\rho}$ is the wave velocity related to the mass density $\rho$ and elastic stiffness constant $C_{44}$, and $\omega$ is the vibrational frequency of the phonon. Here, the values of elastic stiffness constant and mass density for GaAs and AlAs referred to $C_{44}({\rm GaAs}) = 5.99\times10^{10}$ N/m$^2$, $C_{44}({\rm AlAs}) = 5.67\times10^{10}$ N/m$^2$, $\rho({\rm GaAs}) = 5317$ kg/m$^3$, $\rho({\rm AlAs}) = 3760$ kg/m$^3$.[34] The solution for Eq. (2) in each region can be expressed as

$$U^{\xi} = \sum_{m=0}^{\infty}[C^{+}_{\xi m}{\rm e}^{+{\rm i}k^{\xi}_{mz}z} + C^{-}_{\xi m}{\rm e}^{-{\rm i}k^{\xi}_{mz}z}]\phi^{\xi}_m, \tag{3}$$

where $\phi^{\xi}_m$ represents the orthonormal wave functions of the $m$-th mode in region $\xi$, and $C^{+}_{\xi m}$ and $C^{-}_{\xi m}$ are the transmitted and reflected amplitudes of the $m$-th mode in region $\xi$, respectively. Employing the stress free boundary condition $\hat{n}\cdot\nabla\phi^{\xi}_m = 0$ at the edges, we can get

$$\phi^{\xi}_m = \begin{cases} \sqrt{\dfrac{2}{\pi}}\dfrac{r}{r^2_{\xi}}, & m = 0, \\ \sqrt{\dfrac{2}{\pi}}\dfrac{{\rm J}_1(\chi_m r/r_{\xi})}{{\rm J}_1(\chi_m)\chi_m}, & m \neq 0. \end{cases} \tag{4}$$

Here, ${\rm J}_n$ is the $n$-th-order Bessel function of the first kind, and $\chi_m$ is the $m$-th solution of ${\rm J}_2(\chi_m) = 0$. Then we can calculate the transmission coefficient $\tau_m$ by using the scattering matrix method. In the calculations, we take all the propagating modes and several lowest evanescent modes into account to meet the desired precision. For further details of these calculations, see Li *et al.*[35]

## 3. Results and discussion

In Fig. 2, we calculate the total transmission coefficient $\tau_{\rm total}$ as a function of the reduced frequency $\omega/\Delta$ ($\Delta = v/r_1$) for varying radii $r_2$ of the scattering region with different materials. Here, the material in regions I and III is always GaAs. For comparison, the transmission coefficient for an ideal nanowire is also calculated in Fig. 2(a). From the figure, we can find that the $\tau_{\rm total}$ curve shows ideal quantum transmission stepwise platforms that gives the number of the phonon transport channels in the ideal nanowire, indicating that the available phonons can pass completely through this structure without reflection. Note that the breadth of these platforms is nonuniform especially for the first platform, which is different from that in rectangular nanowires.[36] When the material GaAs in region II is substituted by AlAs in a straight nanowire, from Fig. 2(b), $\tau_{\rm total}$ decreases strongly from interface scattering of incident phonons from the acoustic mismatch, the ideal

transmission coefficient is destroyed and becomes blurred especially when the reduced frequency $\omega/\Delta$ is larger than 5. In the presence of the abrupt scattering region in region II, the transmission coefficient further reduces due to the added scatter by the discontinuous abrupt interfaces in Fig. 2.

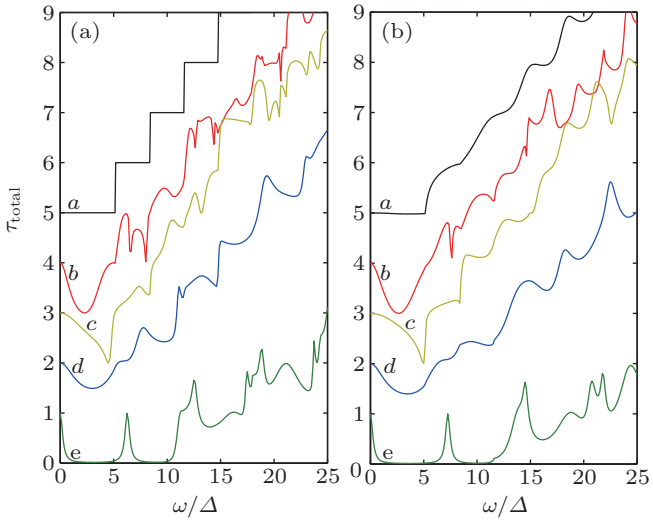



**Fig. 2.** (color online) Total transmission coefficient $\tau_{\rm total}$ as a function of the reduced frequency $\omega/\Delta$ for different radii $r_2$. Panel (a) corresponds to the scattering region with material GaAs and panel (b) corresponds to the scattering region with material AlAs. Curves $a$, $b$, $c$, and $e$ are for $r_2 = 10$, 15, 12, 8, and 5 nm, respectively. Here, we take $r_1 = 10$ nm and $d = 5$ nm. Each curve is vertically offset by unity for clarity.

In the concavity-shaped structure, the transmission coefficient significantly decreases. In the limit $\omega \to 0$, however, all the $\tau_{\rm total}$ values remain unity regardless of the geometric parameters and material properties of the scattering region. This can be well understood, the phonon wavelength $\lambda$ depends on the material wave velocity $\upsilon$ and the phonon frequency $\omega$, which can be expressed as $\lambda = 2\pi\upsilon/\omega$. Here, wave velocity $\upsilon$ is a constant, thus the wavelength $\lambda$ increases as the phonon frequency $\omega$ decreases, meaning that a phonon with extremely long wavelength at $\omega = 0$ is hardly scattered by the discontinuous interfaces. Note that, at $r_2 = 5$ nm, in the low-frequency region, the total transmission coefficient exhibits some stop-frequency gaps, which can be opened and are clearly different from these stemming from the Van Hove singularities of perfect phonon bands. These stop-frequency gaps may be attributed to the antiresonant coupling between the incident waves and reflected waves because of multi-reflection in the scattering region. As the incident frequency increases ($\omega/\Delta > 6$), the stepped profile of the transmission coefficient becomes more distinct, and the number of transmission platforms increases. To understand these behaviors, the cutoff frequency, $\omega_m = \chi_m v/r_2$, needs to be analyzed. When the incident frequency is larger than the cutoff frequency of the $m$-th mode, this mode can be excited to contribute to the phonon transmission. As $r_2$ increases, $\omega_m$ decreases, so more modes can be excited. Thus, the number of the excited modes in the convexity-shaped structure is larger than that in the concavity-shaped structure.

Now, we turn to investigate how the phonon thermal conductance depends on the reduced temperatures and structural parameters. In Fig. 3, we depict the total thermal conductance $K$ as a function of the reduced temperature $T$ for different radii $r_2$. For the straight cylindrical nanowire ($r_2 = 10$ nm), $K$ presents the longer quantum platform in the low temperature range compared to the rectangular nanowire.[36] As the temperature goes up, higher index phonon modes are excited and contribute to the thermal conductance, thus thermal conductance increases monotonously. It is worth pointing out that due to the higher cutoff frequencies in cylindrical nanowires, the magnitude of thermal conductance in cylindrical nanowires is always smaller than the corresponding value in rectangular nanowires at high temperatures.[36] When the abrupt scattering region is emerged in the nanowire, the thermal conductance curve descends markedly due to sudden material and structural changes from the quantum value to a minimum at low temperatures. However, in the limit $T \to 0$, $K$ approaches the universal value $\pi^2 k_{\rm B}^2 T/3h$ for all the cases. This is because an acoustic phonon at $\omega = 0$ can retain the perfect transmission even in the presence of discontinuous interfaces. In Fig. 3(a), for $r_2 = 15$ nm, the thermal conductance of the nanowire with an AlAs convexity region is bigger than that of the nanowire with a GaAs convexity region when the reduced temperature $T$ is smaller than 0.3 K. However, the thermal conductance has an opposite transition trend when $T$ is larger than 0.3 K. This is because the thermal conductance depends largely on the contribution of zero mode at lower temperatures. The acoustic phonon wavelength of the zero mode is $\lambda = 2\pi\upsilon/\omega$, $\upsilon$ is the wave velocity of the material, the wave velocity in AlAs is bigger than that in GaAs, the wavelength $\lambda$ in AlAs is larger than that in GaAs, the phonon with zero mode can easily go through the AlAs convexity region. Thus, the thermal conductance of the nanowire with the AlAs convexity region is bigger than that of the nanowire with the GaAs convexity region. At the higher temperature region, $T > 0.3$ K, higher index modes are excited, the cut-off frequency of the higher index mode is $\omega_m = \chi_m \upsilon/r_2$. The wave velocity in AlAs is bigger than that in GaAs, the cut-off frequency of the higher index mode in AlAs is larger than that in GaAs. Therefore, the number of the higher index mode in AlAs is less than that in GaAs, the thermal conductance of the nanowire with the AlAs convexity region is smaller than that of the nanowire with the GaAs convexity region at the higher temperature region. Furthermore, we can clearly see that the transition temperature is enhanced as the decrease of the convexity region radii $r_2$. In Fig. 3(b), at the lower temperature region, the thermal conductance curves of both the nanowire with the GaAs and AlAs concavity regions are identical. However, at the higher tem-

perature region, the thermal conductance of the nanowire with the AlAs concavity region is smaller than that of the nanowire with the GaAs concavity region.

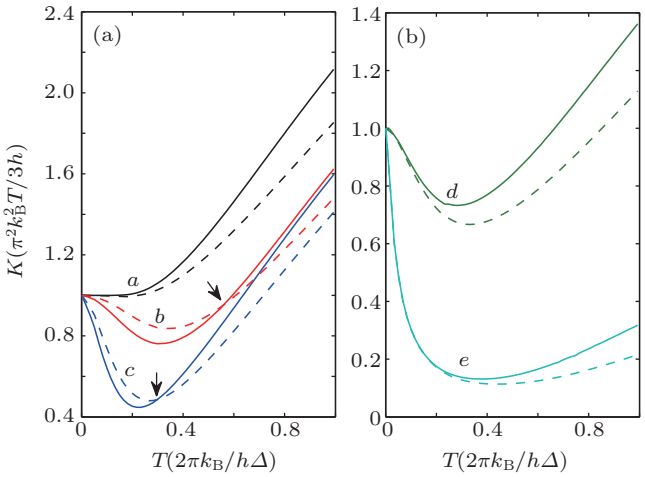



**Fig. 3.** (color online) Total thermal conductance $K$ as a function of the reduced temperature $k_BT/\hbar\Delta$ for different radii $r_2$. Curves $a$, $b$, $c$, $d$, and $e$ are for $r_2 = 10$, 12, 15, 8, and 5 nm, respectively. Solid and dashed curves correspond to the scattering region with material GaAs and AlAs, respectively. The other geometrical parameters are identical to those in Fig. 2.

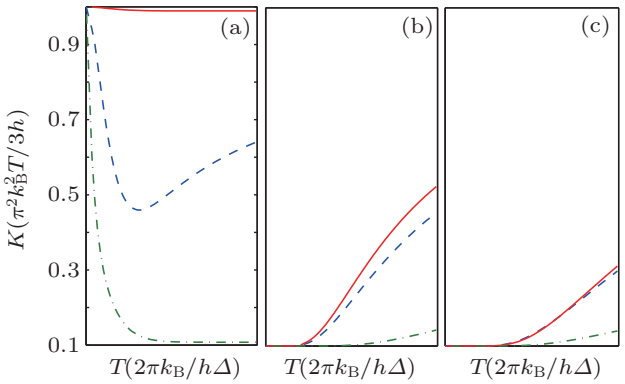



**Fig. 4.** (color online) The thermal conductance $K$ for the three lowest modes as a function the reduced temperature $k_BT/\hbar\Delta$ for different radii $r_2$ of the scattering region with AlAs material. Panels (a), (b), and (c) correspond to the modes $m = 0$, 1, and 2. Solid, dashed, and chain curves correspond to $r_2 = 10$ nm, 15 nm, and 5 nm, respectively. The other geometrical parameters are identical to those in Fig. 2.

In order to further reveal the thermal conductance properties, in Fig. 4, we show the thermal conductance for the individual modes as a function of the reduced temperature for different radii $r_2$. Figures 4(a), 4(b), and 4(c) correspond to the modes $m = 0$, 1, and 2, respectively. It is clearly seen that, for each $r_2$, the thermal conductance reduces as the modal index $m$ increases. This can help explain why only several lowest modes can contribute to the thermal conductance at low temperatures. For the higher modes, their thermal conductance rapidly increases from the zero as the temperature increases. However, the thermal conductance is usually smaller than that of the zero mode, even at higher temperatures. These behaviors indicate that the zero mode plays an important role in determining phonon thermal conductance at low temperatures.

Finally, figure 5 shows the total thermal conductance $K$ as a function of the length $d$ of the scattering region at the temperature controlled area. The results show that, at very low temperatures, $T = 0.2$ K, the total thermal conductance is $\pi^2k_B^2T/3h$ and does not depend on the length $d$ of the scattering region and the material properties in a straight nanowire. This is because the scattering of the scattering region on the acoustic phonon with zero model is very small at very low temperatures. However, at high temperatures, $T = 2$ K, the thermal conductance increases and approaches to $1.5\pi^2k_B^2T/3h$, this is because higher modes are excited and make a contribution to the thermal conductance. Clearly, the scattering region with AlAs material significantly reduces the thermal conductance with the increase of the length $d$, this is from interface scattering of incident phonons from the acoustic mismatch. In the convexity-shaped structure, $T = 0.2$ K, the thermal conductance of the nanowire with the AlAs convexity region is larger than that of the nanowire with the GaAs convexity region; however, $T = 2$ K, the thermal conductance has the opposite trend, this is attributed to the material AlAs with the higher wave velocity. In addition, the thermal conductance curve appears with some peaks and dips at special $d$, due to the intricate transmission behaviors of higher index modes. In the concavity-shaped structure, $T = 0.2$ K, the curves of the thermal conductance for both the nanowire with the GaAs and AlAs concavity region are identical and decrease rapidly in a monotone way, meaning that material properties have less effect on the thermal conductance at very low temperatures; at high temperatures, $T = 2$ K, the thermal conductance decreases rapidly from the fixed value to the minimum and finally holds constant, this is because the interface scattering from discontinuities strongly depresses the phonon transmission.

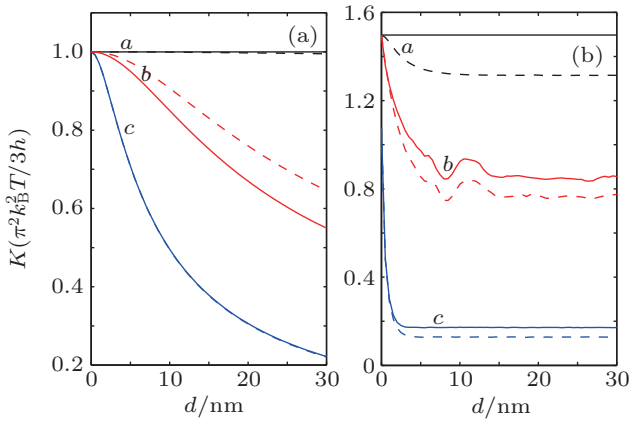



**Fig. 5.** (color online) Total thermal conductance $K$ as a function of the length $d$ of the scattering region for different radii $r_2$ at the temperature controlled area. Panels (a) and (b) correspond to $T = 0.2$ K and $T = 2$ K. Curves $a$, $b$, and $c$ are for $r_2 = 10$, 15, and 5 nm, respectively. Solid and dashed curves correspond to the scattering region with material GaAs and AlAs. Here, we take $r_1 = 10$ nm.

## 4. Conclusions

We have investigated material properties dependent on the thermal transport in a cylindrical semiconductor nanowire by using the elastic wave continuum model. Our numerical results show an interesting physical effect: the behavior of the thermal conductance is different for different types of the scattering region with different types of the material. In the convexity-shaped structure, the material with higher wave velocity in the convexity region can increase the thermal conductance at the lower temperature range; the thermal conductance of the nanowire with higher wave velocity in the convexity region is lower than that of the nanowire with lower wave velocity in the convexity region at the higher temperature range. However, in the concavity-shaped structure, the material properties of the concavity region have less effect on the thermal conductance at the lower temperature range; the material with higher wave velocity in the concavity region can reduce the thermal conductance at the higher temperature range. Moreover, a quantized thermal-conductance plateau can be observed in an ideal cylindrical nanowire. To further study how the scattering region affects the thermal conductance properties, we also studied the individual mode and found that the zero mode plays an important role in determining phonon thermal conductance at low temperatures. Our results suggest that adjusting the structure and material properties of the scattering region may provide a valuable reference for modulating thermal transport in application of nanoscale devices.

## References


[1] Chang C W, Okawa D, Majumdar A and Zettl A 2006 *Science* **314** 1121
[2] Li N, Ren J, Wang L, Zhang G and Li B 2012 *Rev. Mod. Phys.* **84** 1045
[3] Cahill D G, Braun P V, Chen G, Clarke D R, Fan S, Goodson K E, Keblinski P, King W P, Mahan G D, Majumdar A, Maris H J, Phillpot S R, Pop E and Shi L 2014 *Appl. Phys. Rev.* **1** 011305
[4] Ming Y and Ding X 2014 *Chin. Phys. Lett.* **31** 080501
[5] Dubi Y and Ventra M D 2011 *Rev. Mod. Phys.* **83** 131
[6] Zhang G and Li B 2010 *Nanoscale* **2** 1058
[7] Feng Y, Zhu J and Tang D W 2014 *Chin. Phys. B* **23** 083101
[8] Ramin Y, Mohsen C, Farid J S, Mahomoudian M R, Abdolhossein S and Nay M H 2014 *Chin. Phys. B* **23** 108101
[9] Rego L C C and Kirczenow G 1998 *Phys. Rev. Lett.* **81** 232
[10] Schwab K, Henriksen E A, Worlock J M and Roukes M L 2000 *Nature* **404** 974
[11] Duchemin I and Donadio D 2012 *Appl. Phys. Lett.* **100** 223107
[12] Zhang Y, Xie Z X, Yu X, Wang H B and Li K M 2014 *J. Appl. Phys.* **116** 144304
[13] Xie Z X, Zhang Y, Yu X, Li K M and Chen Q 2014 *J. Appl. Phys.* **115** 104309
[14] Lin K H and Strachan A 2013 *Phys. Rev. B* **87** 115302
[15] Zhang G and Zhang Y 2013 *Phys. Status Solidi* **7** 754
[16] Liu Y Y, Zhou W X, Tang L M and Chen K Q 2014 *Appl. Phys. Lett.* **105** 203111
[17] Nie L Y, Li C X, Zhou X P, Wang C Z and Cheng F 2012 *Chin. Phys. B* **21** 026301
[18] Zhu H, Xu Y, Gu B and Duan W 2012 *New. J. Phys.* **14** 013053
[19] Gong W, Zhang W, Ren C, Wang S, Wang C, Zhu Z and Huai P 2013 *RSC Advances* **31** 12855
[20] Mingo N, Stewart D A and Broido D 2008 *Phys. Rev. B* **77** 033418
[21] Yamamoto T, Sasaoka K and Watanabe S 2011 *Phys. Rev. Lett.* **106** 215503
[22] Xie G, Shen Y, Wei X, Yang L, Xiao H, Zhong J and Zhang G 2014 *Sci. Rep.* **4** 5085
[23] Lan J, Cai Y, Zhang G, Wang J S and Zhang Y W 2014 *J. Phys. D: Appl. Phys.* **47** 265303
[24] Ouyang T, Chen Y P, Xie Y, Stocks G M and Zhong J X 2011 *Appl. Phys. Lett.* **99** 233101
[25] Xie Z X, Chen K Q and Duan W H 2011 *J. Phys.: Condens. Matter* **23** 315302
[26] Chen K Q, Li W X, Duan W H, Shuai Z and Gu B L 2005 *Phys. Rev. B* **72** 045422
[27] Hao F, Fang D and Xu P 2011 *Appl. Phys. Lett.* **99** 041901
[28] Shao Z G, Ai B Q and Zhong W R 2014 *Appl. Phys. Lett.* **104** 013106
[29] Huang H, Xu Y, Zou X, Wu J and Duan W 2013 *Phys. Rev. B* **87** 205415
[30] Jiang J W, Wang B S and Wang J S 2011 *Appl. Phys. Lett.* **98** 113114
[31] Pei Q X, Zhang Y W, Sha Z D and Shenoy V B 2013 *J. Appl. Phys.* **114** 033526
[32] Liu B, Reddy C D, Jiang J, Zhu H, Baimova J A, Dmitriev S V and Zhou K 2014 *J. Phys. D: Appl. Phys.* **47** 165301
[33] Huang W Q, Zou M L, Huang G F, Yao J J and Hu W Y 2009 *J. Appl. Phys.* **105** 124305
[34] Madelung O 1982 *Semiconductors: Group IV Elements and III–V Compounds* (Berlin: Springer Press)
[35] Li W X, Chen K Q, Duan W H, Wu J and Gu B L 2003 *J. Phys. D: Appl. Phys.* **36** 3027
[36] Huang W Q, Chen K Q, Shuai Z, Wang L L, Hu W and Zou B S 2005 *J. Appl. Phys.* **98** 093524